Available online at www.sciencedirect.com
SCIENCE DIRECT®
Sedimentary Geology 162 (2003) 39–62
Sedimentary Geology
www.elsevier.com/locate/sedgeo

Muddled or mixed? Inferring palaeoclimate from size distributions of deep-sea clastics

Gert Jan Weltje[a,*], Maarten A. Prins[b]

[a] Department of Applied Earth Sciences, Delft University of Technology, PO Box 5028, NL-2600 GA Delft, The Netherlands
[b] Faculty of Earth and Life Sciences, Vrije Universiteit, De Boelelaan 1085, NL-1081 HV Amsterdam, The Netherlands

Abstract

One of the outstanding problems of palaeoclimate reconstruction from physico-chemical properties of terrigenous deep-sea sediments stems from the fact that most basin fills are mixtures of sediment populations derived from different sources and transported to the site of deposition by different mechanisms. Conventional approaches to palaeoclimate reconstruction from deep-sea sediments do not distinguish between provenance and dispersal-related variations, and therefore often fail to recognise the true significance of variations in sediment properties. We formulate a set of requirements that each proposed palaeoenvironmental indicator should fulfil, and focus on the intrinsic coupling between grain size and chemical composition. A critical review of past achievements in grain-size analysis serves to introduce a conceptual model of spatio-temporal grain-size variation based on dynamic populations. Each dynamic population results from a characteristic combination of production and transport mechanisms that corresponds to a distinct subpopulation in the data analysed. The mathematical–statistical representation of the conceptual model can be obtained by means of the end-member-modelling algorithm EMMA. Applications of the model to several ocean basins are discussed, as well as methods to examine the validity of grain-size-based palaeoclimate reconstructions. Palaeoclimate reconstructions of a high- and low-latitude basin illustrate the common degree of complexity of deep-sea grain-size records.

Keywords: Mixtures; End-member modelling; Grain-size distribution; Dynamic population; Palaeoclimate; Deep-marine sediments

1. Introduction

Cores of Late Quaternary deep-sea sediments provide accurately datable continuous records from which the coupled evolution of continental and oceanic environments may be reconstructed. Deep-sea sediments comprise biogenic components of dominantly intrabasinal origin and a terrigenous fraction that reflects the supply of sediments produced on adjacent continents. Specialised chemical and micropalaeontological analyses of the biogenic fraction of deep-sea cores have significantly deepened the insights into palaeoceanographic evolution. The terrigenous fraction of deep-sea sediments lends itself to routine analysis by means of core scanners, laser particle sizers and comparable devices. It represents the chief source of information on weathering conditions in sediment source areas and on palaeoatmospheric circulation. In addition, it may be used

* Corresponding author. Tel.: +31-15-2785722; fax: +31-15-2781189.
E-mail addresses: g.j.weltje@citg.tudelft.nl (G.J. Weltje), prim@geo.vu.nl (M.A. Prins).

0037-0738/$ - see front matter © 2003 Elsevier B.V. All rights reserved.
doi:10.1016/S0037-0738(03)00235-5

to reconstruct variations in palaeoceanographic circulation. Considerable efforts have been made to extract palaeo-environmental information from physico-chemical sediment properties such as magnetic susceptibility, grain-size distribution (GSD), and mineral/chemical composition. The ultimate aim of these methods is to identify sediment properties that are convenient to measure and carry the palaeo-environmental signals of interest, often referred to as 'proxies.' The main purpose of this contribution is to discuss how palaeoclimate information can be extracted from GSDs of deep-sea clastics.

The idea that GSDs may provide valuable information on provenance and dispersal of sediments has great intuitive appeal, and consequently, a wide range of methods to extract genetic information from this type of data has been proposed. However, existing methods of analysing grain-size variation are based on restrictive assumptions, and of limited use as palaeo-environmental tools. A generic approach to the use of grain size as palaeo-environmental indicator requires that spatio-temporal patterns of grain-size variation can be characterised in a way that is both objective and genetically meaningful. We introduce a conceptual model of the significance of grain-size variation in deep-sea clastics that is consistent with the basic requirements for useful palaeo-environmental indicators. The corresponding mathematical model is obtained by inversion of grain-size data with EMMA, the numerical–statistical end-member-modelling algorithm developed by Weltje (1997, 2001). Models based on data sets from various ocean basins will be presented (Fig. 1). In addition, we discuss comparisons of modelling results to independent sources of information, and general problems of palaeoclimate reconstruction from grain-size data.

1.1. Basic requirements of palaeo-environmental indicators

The usefulness of any palaeo-environmental indicator is determined by the quality of the measurements and the process-response model that relates the measurements to the palaeo-environmental signal of interest. An operational definition of the quality of measurements should be based on the notion of reproducibility, which reflects the spatial scale (areal extent) and temporal resolution of the palaeo-environmental reconstruction, and not simply the analytical error of the measurement procedure. This requirement is difficult to meet in practice (suggestions to take a replicate deep-sea core are treated with ridicule in many circles), but attention should at least be given to estimation of the random component in the data to minimise the danger of overspecification.

A process-response model of the system under study is required to motivate the palaeo-environmental significance of an indicator. The (postulated) causal relationship between changes in the environmental variable of interest and changes in the measured sediment property must of course be plausible, i.e., based on commonly accepted theory and facts. By far, the most important requirement is that this relationship must be monotonic, which only holds if changes in the measured property exclusively reflect changes in the variable of interest. Any indicator fulfilling these requirements can be used to make predictions that may be examined in the light of independent evidence, i.e., other types of data from the same locality/core, or the same type of data from other localities/cores.

An illustration of the complicated interpretation of sediment properties that do not show a unique monotonic relationship with a single environmental variable is provided by the bulk magnetic susceptibility (BMS) of sediment cores from the North Atlantic and the Arabian Sea (Fig. 2). Interpretation of the BMS of mixed carbonate-siliciclastic deposits is possible under the assumption that the composition of the siliciclastic fraction in a core is more or less constant. In such case, the BMS may be interpreted as the mirror image of the carbonate content. Another possibility is that the carbonate content of the core is more or less constant, in which case the BMS signal reflects size/composition variation within the terrigenous fraction. As the exact nature of this variation cannot be determined from the BMS signal alone, it cannot be interpreted in palaeo-environmental terms without additional information. In practice, the BMS record rarely provides a straightforward palaeo-environmental indicator, because both the carbonate content and the composition of the terrigenous sediment fraction are expected to vary over long time intervals (Fig. 2), due to changes in sediment production and supply patterns.

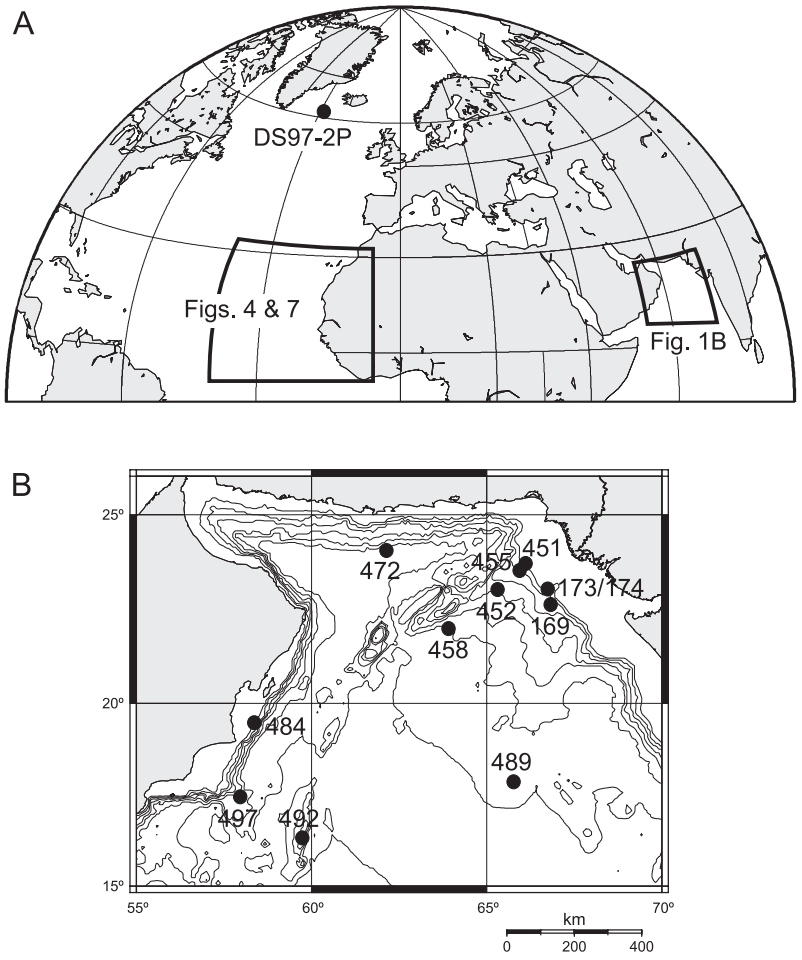

Fig. 1. Location of marine sediment cores used in this study.

Similar problems are associated with the use of many other univariate indicators, such as chemical element ratios and univariate GSD parameters. Fig. 3A shows the downcore variation in grain size and bulk chemical composition (log{Ca/Al} and log{Ti/Al}) within a single turbidite bed from the Indus Canyon valley floor. The scatter plots of Fig. 3B suggest geochemical characterisation of grain size to be straightforward, as both log ratios exhibit nearly monotonic trends with median size. However, chemical analysis of narrow size fractions of a sample from the top of the bed does not show such a monotonic relation. This illustrates that the bulk geochemical signature reflects the entire GSD of the samples, and not simply the median grain size within a given turbidite interval. Hence, one should be careful to draw conclusions about grain size on the basis of bulk chemistry alone. Inferences about sediment provenance and the mode of sediment transport from bulk chemistry are even more error-prone. Univariate indicators can only be used with confidence if their local palaeo-environmental significance has been firmly established.

1.2. Grain size as palaeo-environmental indicator

Many attempts to extract palaeo-environmental information from terrigenous deep-sea sediments have

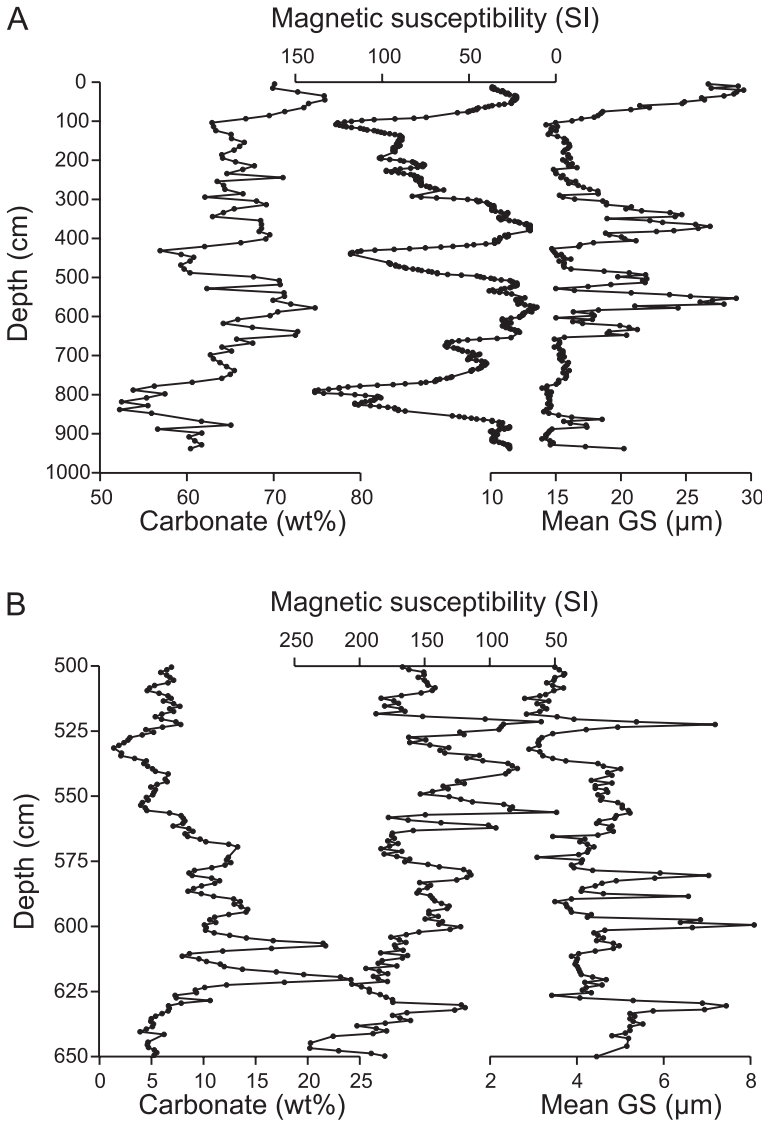

Fig. 2. Magnetic susceptibility records of (A) core NIOP492 from Owen Ridge, Arabian Sea, and (B) core DS97-2P from Reykjanes Ridge, North Atlantic, compared to bulk carbonate content and mean grain size of the siliciclastic fraction. Note reversed scales of the magnetic susceptibility records. Data from Prins and Weltje (1999) and Prins et al. (2001).

focused on the use of variations in univariate summary statistics such as the median, mean, sorting or skewness of GSDs. This approach to characterisation is unlikely to be successful because most deep-sea siliciclastics are mixtures of different sediment types, as a consequence of time-averaging effect related to bioturbation and low accumulation rates. On a global scale, dominant constituents of deep-sea clastics are pelagic components brought in by the wind and hemipelagic components derived from fluvial and shelfal sources. Other types of deep-sea deposits, such as turbidites, contourites, and glacio-marine detritus are not nearly as areally extensive as hemipelagites, but may be of considerable regional importance.

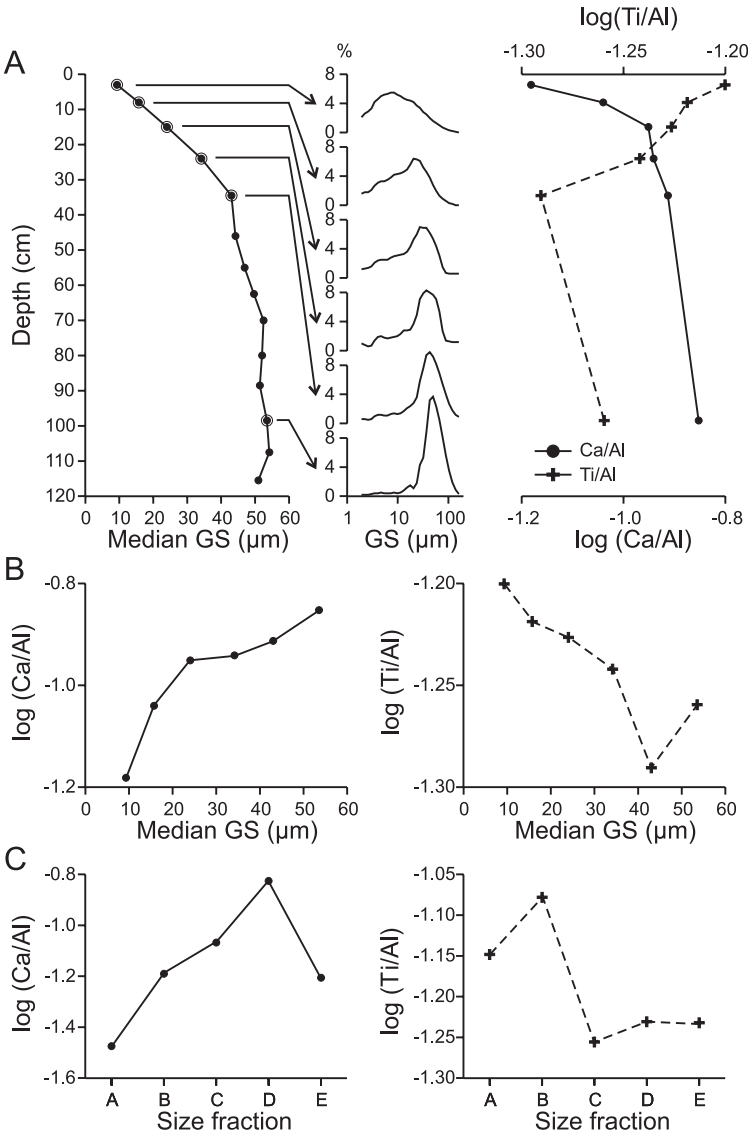

Fig. 3. Grain-size variation and chemical composition in a turbidite interval in core SO90-174SL, Indus canyon, Arabian Sea. (A) Median grain size, grain-size distributions and bulk chemical composition of selected samples. (B) Scatter plots of median grain size and bulk chemical composition. (C) Chemical composition of narrow size fractions from surface sediment sample in neighbouring boxcore SO90-173KG. Silt fractions A, B, C, and D have modal grain sizes of ~ 2, ~ 5, ~ 15, and ~ 40 μm, respectively, and sand fraction E contains particles >63 μm. Data from Prins et al. (2000a).

Temporal changes in the fluxes of most sediment types may be interpreted in palaeo-environmental terms. For instance, the flux of river-derived fine-grained siliciclastics (suspension load) is expected to correlate with continental runoff and may be used as a palaeo-humidity indicator. Analysis of aeolian dust allows estimation of the palaeo-aridity of aeolian source regions via flux determinations, and of the intensity of the transporting winds from grain-size measurements. The flux of ice-rafted detritus (IRD) is

expected to correlate with the discharge of icebergs to the open marine environment, and the grain size of contourite deposits reflects the intensity of near-bottom currents. Hence, both may be used as indicators of ocean circulation. Turbidite fluxes may also be indicative of specific palaeo-climate conditions, for instance in cases where they reflect the frequency of hyperpycnal flows generated during extreme fluvial discharge events.

An obvious consequence of the above is that one cannot interpret variations within the terrigenous fraction in terms of palaeoclimate variation without knowledge of the provenance, the dispersal pathways and the transport mechanisms of the sediments under consideration. In the absence of such knowledge, provenance and dispersal of the terrigenous fraction form an intrinsic part of the problem of palaeoclimate reconstruction that cannot be ignored. Therefore, the fundamental problem that faces marine geologists and paleoceanographers in their search for accurate palaeo-environmental indicators is to determine whether the measured grain-size variation should be attributed to mixing of detritus from multiple sources, to size-selective dispersal, or to some combination of both.

2. A brief history of grain-size analysis

2.1. Distribution functions

Grain-size analysis took off in the 1930s with the introduction of the phi-size scale (Krumbein, 1934), which popularised the lognormal model of mass-size distribution. It was soon discovered that systematic deviations from lognormality appear to be the rule rather than the exception (Tanner, 1958), and various alternative distribution functions were proposed. The Weibull (or Rosin) distribution is among the most popular of these (Kittleman, 1964; Ibbeken, 1983; Kondolf and Adhikari, 2000), with the log-hyperbolic distribution as a strong contender (Bagnold and Barndorff-Nielsen, 1980; Christiansen and Hartmann, 1991; Hartmann and Christiansen, 1992). All of the above GSDs, as well as several other ones can be derived from probability considerations (Middleton, 1970; Dapples, 1975; Dacey and Krumbein, 1979; Barndorff-Nielsen and Christiansen, 1988; Ghosh, 1988; Fieller et al., 1992; Kondolf and Adhikari, 2000). A comprehensive physical theory of sediment-size distribution is not yet available, although process-based models have been proposed for specific settings (Ghosh and Mazumder, 1981; Wohletz et al., 1989; Kranck et al., 1996a,b).

Many researchers have attributed departures from lognormality to mixing of elementary distributions, inspired by early studies of Doeglas and Brezesinska Smithuysen (1941) and Doeglas (1946), who observed that many cumulative GSDs drawn on arithmetic probability paper appear to be composed of several nearly straight line segments separated by 'breaks.' They argued that such curves represent mixtures of Gaussian (normal) distributions that correspond to so-called reference sediment types. Visher (1969), Middleton (1976), and Bridge (1981) discussed possible functional forms of subpopulations in the light of their hydrodynamic significance. Subsequent studies have shown that such 'breaks' between straight line segments in cumulative grain-size plots emerge whenever non-lognormal distributions are plotted on paper with a lognormal cumulative probability scale, which implies that graphic methods of hydraulic interpretation cannot be trusted (Leroy, 1981; Christiansen et al., 1984; Komar, 1986). Similar attempts to resolve GSDs into contributions of elementary populations represented by individual laminae did not lead to unequivocal conclusions (Grace et al., 1978; Emery, 1978).

The common occurrence of deposits with polymodal GSDs is a compelling argument for the existence of distinct subpopulations, as first demonstrated by Folk and Ward (1957) and discussed in more detail by Ashley (1978) and Flemming (1988). Estimation of the components, usually assumed to be lognormally distributed, has been attempted by means of various analytical, graphic and numerical approaches (Clark, 1976). An early example of a graphic approach to the mixing problem is the paper by Curray (1960), who manually decomposed polymodal frequency distributions into a series of lognormal distributions by a subtractive method. Sheridan et al. (1987) and Shih and Komar (1994) presented numerical versions of this procedure. A recent variation on this theme is the method advocated by Sun et al. (2002), who proposed a decomposition of polymodal GSDs into Weibull (Rosin) distributions. A more process-based approach

is provided by Wohletz et al. (1989), who advocated a decomposition of polymodal GSDs into mixtures of so-called sequential fragmentation and transport (SFT) distributions.

A disturbing fact that cannot be ignored is that the number of possible combinations of elementary distributions that could be used to generate a given polymodal GSD is infinite. This nonuniqueness reflects the impossibility of simultaneously inferring the number and the functional forms of the elementary distributions from analysis of one polymodal GSD. Therefore, the usual strategy is a so-called parametric approach: one assumes a functional form and derives the minimum number of elementary distributions from some goodness-of-fit (i.e., reproducibility) measure. In many cases, this may not be desirable given our incomplete understanding of the mechanisms governing the GSD of natural sediments. In the worst case, such a parametric approach could even obscure the existence of genetically significant subpopulations with GSDs differing markedly from one of the popular theoretical models (e.g. Fillon and Full, 1984; Wohletz et al., 1989). Indeed, any type of elementary GSD is conceivable in view of the potentially unlimited number of combinations of initial and acquired grain-size characteristics of natural sediments.

2.2. Multivariate techniques

The oft-cited paper by Folk and Ward (1957) illustrated that recognition of subpopulations of polymodal GSDs requires the analysis of a series of samples from the same depositional environment, in accordance with the views expressed earlier by Doeglas and Brezesinska Smithuysen (1941) and Doeglas (1946). The general principle adopted by these authors is that the variability among observed polymodal size distributions is constrained by the number of subpopulations and their shapes. The next logical step is to explain the observations as mixtures of end-member samples, hand-picked from a set of measured GSDs (Rea and Hovan, 1995; Kurashige and Fusejima, 1997; Boven and Rea, 1998; Orpin and Woolfe, 1999). Possible subjectivity in this form of analysis may be avoided by employing multivariate classification techniques to exploit the information contained within series of genetically related GSDs.

Instead of regarding GSDs as continuous functions, one may consider the proportion of mass in each size class to be an attribute of a multivariate observation. According to this view, each GSD is a single datum, comprising as many components as there are size classes. Many multivariate methods attempt to capture the relations between the observations that make up a data set, whereas other methods subdivide a data set into groups of observations with similar overall characteristics. In contrast with the previous methods, the functional forms of the groups, clusters, or end members do not have to be specified beforehand. Multivariate methods are therefore nonparametric with respect to the shapes of the GSDs of each subpopulation. Multivariate approaches to the recognition of subpopulations in grain-size data include cluster analysis (Zhou et al., 1991) and entropy analysis (Forrest and Clark, 1989). However, the multivariate techniques used most extensively for this purpose are principal components analysis (e.g. Davis, 1970; Chambers and Upchurch, 1979; Lirer and Vinci, 1991; Zhou et al., 1991) and factor analysis (e.g. Klovan, 1966; Solohub and Klovan, 1970; Allen et al., 1971, 1972; Dal Cin, 1976; Sarnthein et al., 1981; East, 1985, 1987; Syvitski, 1991).

Principal components analysis and factor analysis involve decomposition of the data into: (1) a matrix of ‘components’ or ‘factors’ from which inferences may be drawn about the shapes of the GSDs of each of the groups recognised in the data, and (2) a matrix of ‘loadings’ representing the extent to which each of the input GSDs matches each of the components or factors (Jöreskog et al., 1976; Davis, 1986). Hence, interpretation of subpopulation properties is usually based on the former, and classification of the observations on the latter. A major problem with both techniques is that the results may be difficult to interpret because they cannot be expressed in physical terms. For instance, typical input variables such as mass fractions may have been miraculously transformed to negative values in a component or factor matrix. The reason for this is that principal components and factor analysis were not designed to deal with compositions, i.e., data that are subject to nonnegativity and constant-sum constraints. This is unfortunate because the predominant application of these techniques in sedimentology has been directed towards unmixing of polymodal GSDs. The desire to

unravel compositions in a physically meaningful way has been the motivation for the development of end-member modelling (Weltje, 1997).

3. Grain-size variation in ocean basins

3.1. Dynamic populations

In oceanic basins surrounded by continental source areas, one expects each GSD measured at a given space–time coordinate to represent a mixture of sediment populations corresponding to different mechanisms of production and/or transport. Both groups of processes tend to be selective: they favour certain grain sizes and therefore contribute to fractionation of sediments into distinct grain-size ranges. In our conceptual model of spatio-temporal grain-size variation, each grain-size range corresponding to a characteristic combination of processes is termed a dynamic population (DP). Conversely, a DP may be defined in probabilistic terms as an assemblage of grains that are likely to occur together because they respond in a similar way to the dynamics of sediment production and dispersal within the system. Hence, each sediment sample from a deep-sea basin most likely contains multiple DPs, due to time-averaging effects of bioturbation in conjunction with low accumulation rates of most deep-sea sediments.

The DP provides a plausible link between the grain-size variation observed in cores and palaeoenvironmental reconstructions, because it can be coupled with the physical laws that govern sediment production and transport. The concept of a DP is nonparametric, i.e., it does not imply a particular class of distribution functions. However, we can make a more general assumption about the likely shapes of DPs, based on the fact that one single selection step in the chain of events preceding final deposition is sufficient to produce fractionated sediments, and persistent selection will result in a unimodal GSD regardless of initial conditions. In the case of DPs corresponding to a selective transport mechanism, one expects the upper and lower size limits of their unimodal GSDs to be determined by the dynamics of the transporting medium. If all materials that can be entrained are indeed available in the source area, the upper limit of the GSD corresponds to the largest clasts that can be moved, implying that another, coarser-grained DP remains behind as a lag deposit. The lower limit of the GSD reflects the transition from the selective transport mode of the DP under consideration to a finer-grained DP that need not be transported by the same mechanism. In practice, DPs tend to overlap, indicating that grains of a given size may have been produced by different mechanisms and in various modes.

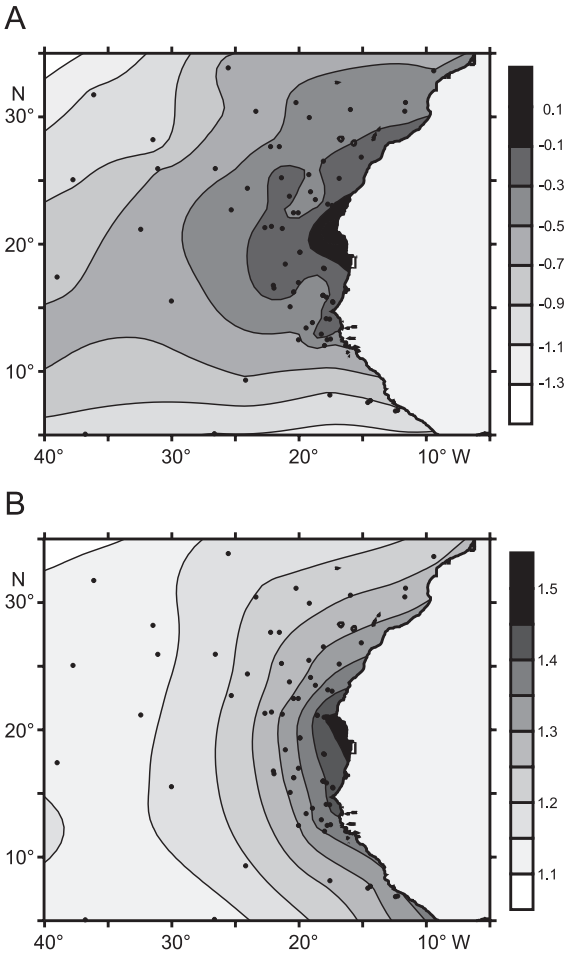

Fig. 4. Spatial variation of grain size in surface sediments offshore NW Africa. Core locations indicated by black dots. (A) Log ratio of contributions of coarse fraction ('aeolian dust' >6.3 μm) to fine fraction ('fluvial mud' < 6.3 μm). (B) Logarithm of median grain size (μm) of the 'aeolian dust' fraction. Raw data and interpretation from Koopmann (1979).

One could distinguish as many different DPs as required to achieve the desired level of detail in sediment characterisation. The limiting case would be to consider each measured grain-size class as a separate DP. In practice, only DPs capable of representing a significant proportion of the basin fill under study are considered useful, because they allow a compact description of the observed grain-size variation. On temporal and spatial scales relevant to changes in global circulation patterns, it is the rule that multiple DPs are associated with a single source area. At least two DPs are needed to represent spatial variation in GSDs resulting from selective dispersal. For instance, a proximal-to-distal fining trend in sediments from a single source (Fig. 4) can be described as mixing of a coarse and a fine DP. The relative contributions of the two DPs to the local GSD are expected to vary systematically in space. In addition, GSDs of sediments shed by a single source over a long period of time may exhibit systematic variations. Such sources are associated with multiple DPs indicative of the extreme conditions in the source area. Hence, a substantial number of DPs may be required to describe the spatio-temporal pattern of grain-size variation in a basin with multiple sediment sources.

The palaeo-environmental significance of grain-size variation in deep-sea basins becomes evident if it can be expressed in terms of mixing of a limited number of DPs, and each DP can be tied to a specific source and dispersal mechanism. Under these conditions, flux ratios of one DP to another should exhibit monotonic relationships to palaeo-environmental variables. For instance, the flux ratio of aeolian to hemipelagic DPs in a deep-sea core could be used as a local measure of aridity, whereas the flux ratio of coarse to fine aeolian DPs could be used to represent wind strength (cf. Prins and Weltje, 1999).

3.2. End members

The mathematical equivalent of the conceptual model presented above is obtained by regarding the measured GSDs as a series of mixtures. The end members (EMs) of the mixing series may then be interpreted as DPs. The typical problem to be solved in applications of grain-size analysis to palaeo-environmental reconstructions is to estimate the number of EMs and their shapes, in order to characterise the mixing structure of the basin fill. This so-called explicit mixing problem can be solved with EMMA, the End-Member Modelling Algorithm (Weltje, 1997, 2001). The resulting mixing model is subject to strict nonnegativity and constant-sum constraints on EM compositions and mixing coefficients to ensure physical interpretability of the model parameters. The

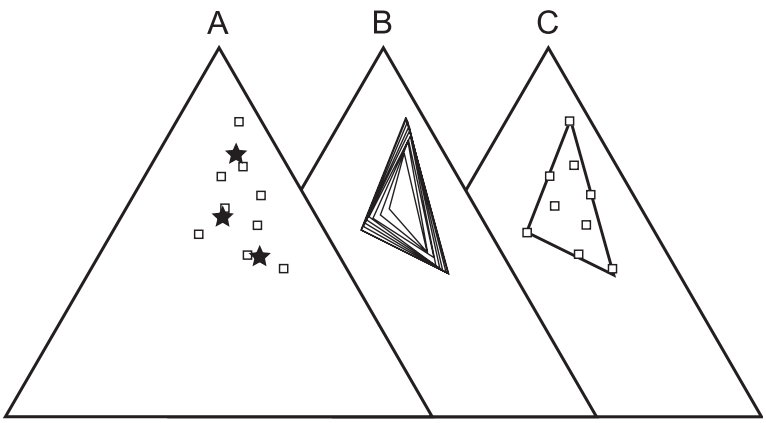

Fig. 5. Construction of a ternary mixing model for a synthetic data set composed of three variables to illustrate the second modelling stage of EMMA. Data set includes the true end members from which the mixtures were generated. (A) Data points (squares) and initial end members (stars). (B) Series of iterations in which the mixing space is expanded. (C) Modelled end members (vertices of the mixing space) closely approximate the true end members at convergence (Weltje, 1997).

assumptions used to derive a mixing model from a series of compositions are:

- The order of the compositional variables or categories is irrelevant (permutation invariance);
- The observed compositional variation reflects linear mixing or an analogous process with a superimposed measurement error;
- The EM compositions are fixed;
- The EM compositions are as close as possible to observed compositions;
- The EMs are linearly independent, i.e., none of the EMs can be expressed as a mixture of the other EMs.

The last assumption is required to estimate the number of EMs independently of their compositions, which constitutes the first step in the modelling process. In the second step, the EM compositions are estimated with an iterative procedure, as illustrated in Fig. 5. EMMA provides a concise description of the observed variation, owing to the fact that it can only identify EMs if their mixing coefficients vary across a series of measured GSDs. This automatically implies that the average contribution of EMs to a basin fill must be volumetrically significant. It must be stressed that EMMA uses no assumptions that are case specific, i.e., it does not require information about the likely shapes of end-member GSDs. In conclusion, the EMs calculated by EMMA correspond in every aspect to the DPs discussed above. Weltje (1997, 2001) covers the technical aspects of EMMA in more detail.

4. Modelling results

4.1. Interpretation and validation

A general consideration with respect to the interpretation of end-member GSDs calculated with EMMA is the so-called permutation invariance of the model. Because EMMA was designed to process categorical data, such as mineralogical and chemical compositions, the order of the grain-size classes is irrelevant to the modelling results. To fully appreciate this, one should think of the grain-size classes as different colours. It does not matter whether one characterises the composition of a jar filled with marbles in terms of (red, white, blue) or one of its possible permutations, say (blue, red, white). In cases where the variables are not categorical, but discretised continuous variables such as grain size, the order of the classes is uniquely defined and the shapes of the end-member GSDs themselves provide additional information about the reasonableness of the conceptual model of grain-size variation. The fact that most end-member GSDs calculated by EMMA turn out to be unimodal is a direct confirmation of our conceptual model.

A set of EMs may be linked to specific source areas or mechanisms of production and dispersal by a variety of methods, which are based on additional information about the data being analysed, such as the core lithology and the order of the samples in space–time. In many cases, independent information is available in the form of samples of known origin, which provide a reality check of the model. Moreover, the intrinsic coupling of sediment size and composition may be used to predict one from the other. Weltje (1995) conducted a similar series of tests of a petrographic end-member model of beach sands in the Northern Adriatic Sea.

4.1.1. Core lithology

Comparison of downcore mixing coefficients of a set of EMs to core lithology is a logical first step in model evaluation, which allows the identification of transport and deposition mechanisms of core intervals in which certain EMs dominate. Prins et al. (2000b) presented an end-member model for the Late Glacial and Holocene sediments of the Makran continental margin, SW Pakistan (Fig. 6). The studied cores are dominated by thinly bedded, fine-grained turbidite successions. Detailed grain-size analysis of two 30–40-cm-thick turbidite beds in core NIOP472 indicates that the median grain size in both sediment beds decreases systematically from base to top. The repeated fining-upward trends, which are evidently related to selective suspension fallout and deposition from turbidity currents, are described by systematic variations in the relative contributions of three end members. For example, the coarse EM-1 is abundant in the basal units of the turbidites and nearly absent in their upper parts, indicating that EM-1 is a turbidite silt–sand.

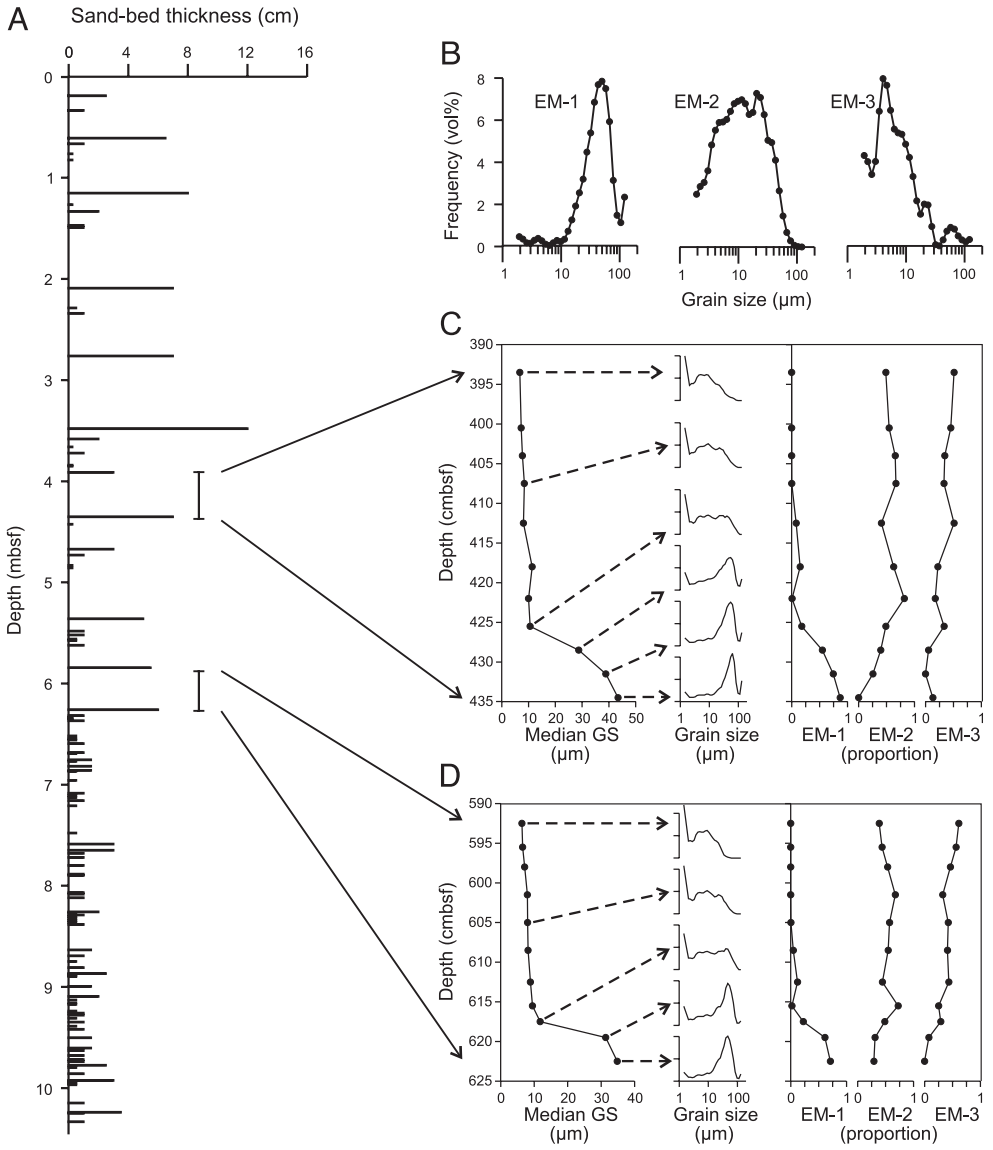

Fig. 6. Lithology and grain-size variation in core NIOP472, Makran margin, Arabian Sea. (A) Turbidite sand-bed thickness and downcore distribution. (B) End-member grain-size distributions. Interpretation: EM-1 = turbidite sandy silt; EM-2 = turbidite mud; EM-3 = hemipelagic mud. (C) and (D) Grain-size variations in two turbidite intervals: median grain size, GSDs of selected samples indicate exact nature of the grain-size variations, proportional contributions of the end members reflect major grain-size trends. Data from Prins et al. (2000b).

4.1.2. Spatial distribution

The source areas and dispersal patterns of EMs can be deduced from the spatial distribution of log ratios of mixing coefficients, as exemplified in Fig. 7. The grain-size variation in aeolian sediments offshore NW Africa (Koopmann, 1979) has been captured with three EMs, in terms of ratios of mixing coefficients that display systematic proximal-to-distal fining trends and allow identification of the source region. Random spatio-temporal distributions of mixing coefficients may indicate that physical mixing of EMs is not a viable hypothesis.

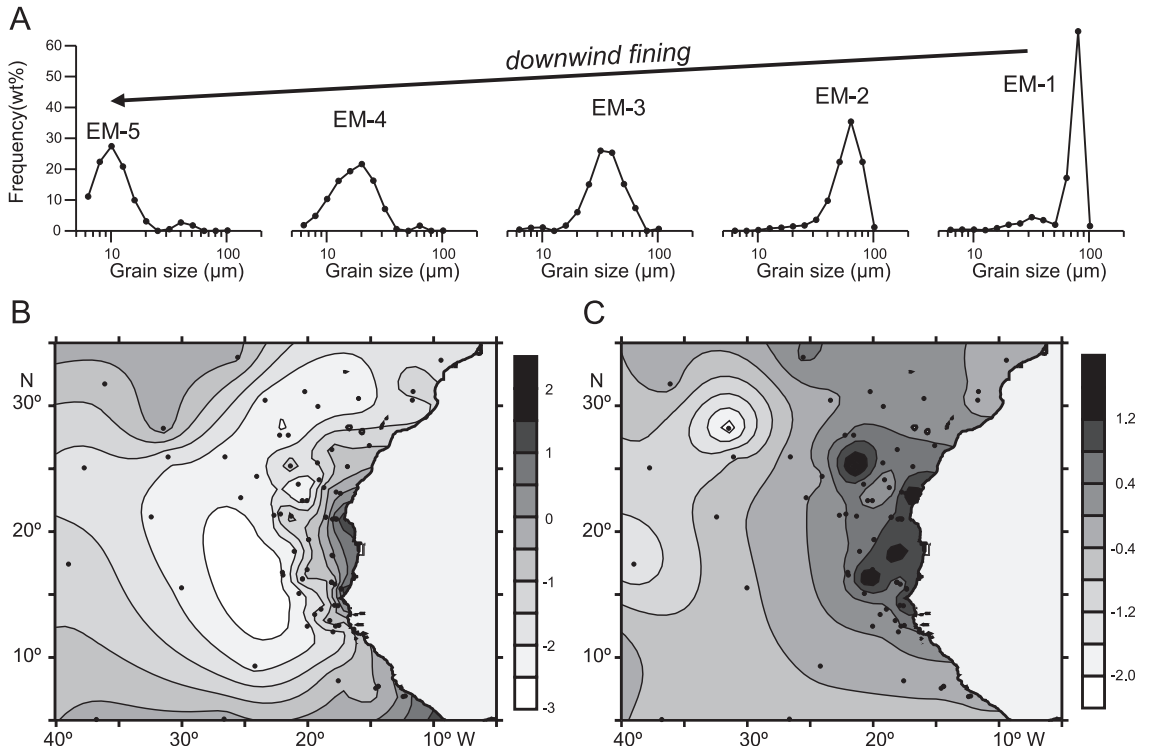

Fig. 7. Spatial variation of end-member contributions in surface sediments offshore NW Africa. Core locations indicated by black dots. (A) End-member grain-size distributions. EM-1 and EM-2 are exceptionally coarse aeolian sediments that occur in a few proximal localities only. EM-3, EM-4 and EM-5 reflect 'coarse', 'medium' and 'fine' aeolian dust. (B) Contour map of log(EM-3/EM-4). (C) Contour map of log(EM-4/EM-5). Raw data from Koopmann (1979).

4.1.3. Reference GSDs

The EMs may be compared to sediments of known origin to infer their genetic significance. Stuut et al. (2002) and Moreno et al. (2002) compared their EMs of presumably aeolian origin to aeolian dust samples collected with sediment traps in their study areas. Moreno's aeolian EM and the trapped aeolian dust are shown in Fig. 8A. Fig. 8B illustrates a similar comparison of a coarse-grained aeolian EM from the Arabian Sea (Prins and Weltje, 1999) with two typical GSDs of Late Quaternary loess from China and Tajikistan (Vandenberghe, unpublished data). Fig. 8C shows two muddy hemipelagic EMs from the Arabian Sea (Prins and Weltje, 1999) and the Makran continental margin (Prins et al., 2000b) together with a typical GSD of fluvial mud deposited on the Indus Fan (Prins et al., 2000a). A comparison between the ice-rafted EM from the North Atlantic and two glacial till samples (Prins et al., 2001, 2002) is given in Fig. 8D.

4.1.4. Chemical composition

An end-member GSD model may be tested by chemical analyses of narrow size fractions, which provide transport-invariant measures of sediment composition in which effects of selective transport due to variations of grain shape and density can be ignored (Weltje, 1998). The transport-invariant composition is by definition independent of the GSD of the sediment. In contrast, the bulk composition is usually a function of the GSD because each size fraction has a characteristic compositional fingerprint (cf. Fig. 3). Use of a transport-invariant measure of sediment composition allows one to distinguish effects of selective transport from those of mixing,

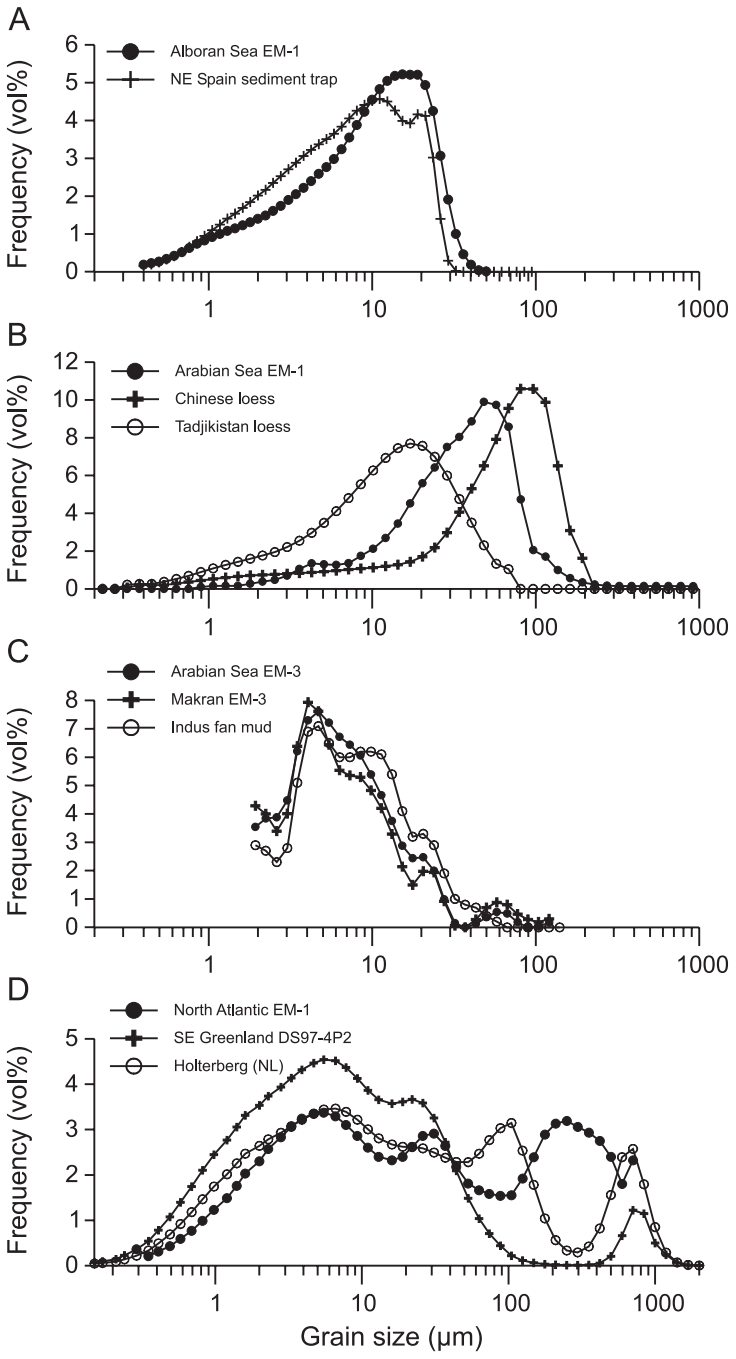

Fig. 8. (A) Aeolian end member from the Alboran Sea, compared to a present-day Saharan dust sample collected in the Montseny Mountains, NE Spain (Moreno et al., 2002). (B) Aeolian end member EM-1 from the Arabian Sea (Prins and Weltje, 1999), compared to two typical loess samples from Tajikistan (Vandenberghe, unpublished data). (C) Hemipelagic/fluvial mud end members EM-3 from the Arabian Sea (Prins and Weltje, 1999) and the Makran margin (Prins et al., 2000b) compared to a typical Indus Fan fluvial mud (Prins et al., 2000a). (D) Ice-rafted detritus end member EM-1 from the North Atlantic (Prins et al., 2001, 2002) compared to two glacial tills collected near Holterberg, Netherlands (Saalien ice-pushed moraines) and from core DS97-4P2 off SE Greenland (Kuijpers et al., 2003).

as shown by Prins et al. (2000a) in their study of the late Quaternary record from the Indus Fan.

Core NIOP489 from the Indus Fan consists of a sequence of silty–sandy turbidites draped by a very homogenous hemipelagic mud unit deposited during the last glacial period, in turn overlain by a calcareous ooze unit of Holocene age (Fig. 9). End-member modelling of the siliciclastic GSDs (Prins and Weltje, 1999) suggested that the sharp increase in grain size during the postglacial sea-level rise reflects the shift from dominantly fluvial to aeolian supply. The end-member GSD model was tested by chemical analysis of three narrow silt-size ranges (fractions B, C and D with modal sizes of ~5, ~15 and ~40 μm, respectively) of sediment samples. The provenance of these Indus Fan samples was inferred by comparison with a series of Holocene reference samples from cores taken at the Oman continental margin (core NIOP484: Arabian aeolian source) and the Indus Canyon (core SO90-173KG: Indus fluvial source). The ternary Al–Mg–Ti subcompositions of all analysed fractions are plotted in Fig. 9. The silt fractions extracted from the turbidite and hemipelagic mud samples of core NIOP489 are chemically identical to the Indus Canyon samples, and are therefore grouped together as 'Indus source' samples in Fig. 9. This compositional similarity indicates that the turbiditic and hemipelagic sediments of the middle Indus Fan were ultimately derived from the Indus River. The silt fractions extracted from the Holocene calcareous ooze unit of the Indus Fan have intermediate compositions with respect to the Arabian-sourced and the Indus-sourced sediments, corroborating the end-member GSD model which indicated that the siliciclastic

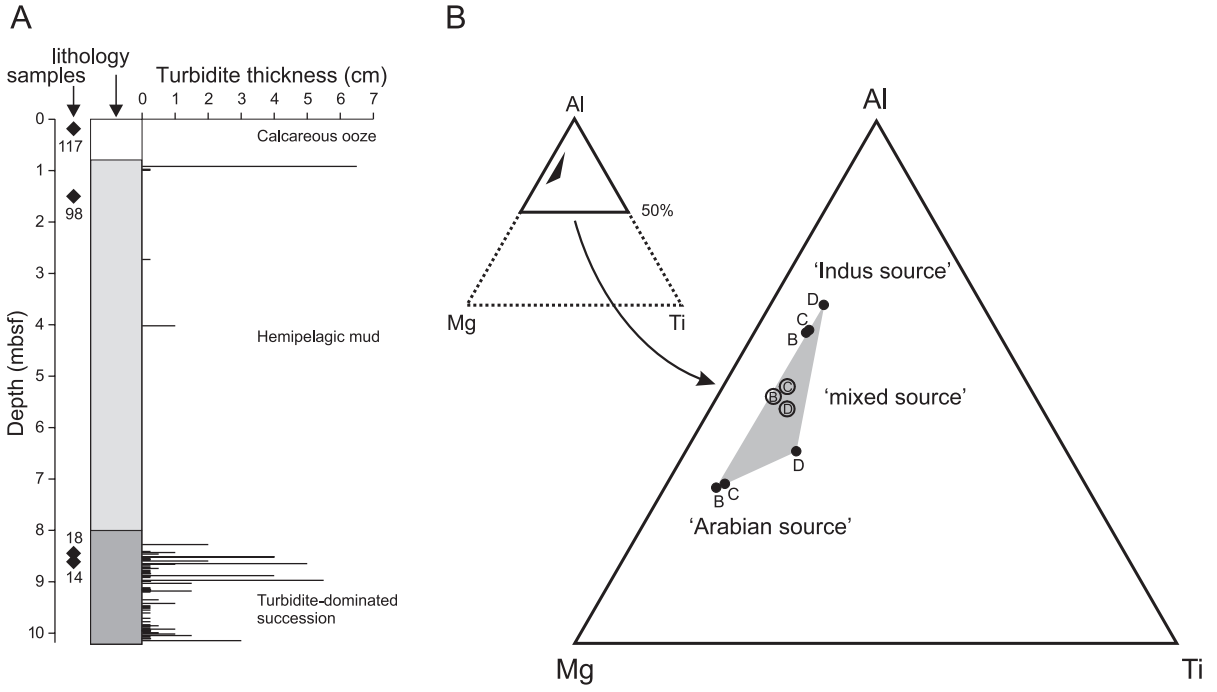

Fig. 9. Provenance of Indus Fan sediments. (A) Lithology in core NIOP489, Indus Fan, Arabian Sea. Position of samples is indicated. (B) Al–Mg–Ti compositions of narrow size fractions B, C, and D with modal grain sizes of ~5, ~15 and ~40 μm, respectively, of sediment samples from the Oman continental slope (core NIOP484: 'Arabian source') and from the Indus Canyon (SO90-173KG: 'Indus source'). Turbidite samples (NIOP489/14 and 18) and a hemipelagic mud sample (NIOP489/98) from the Indus Fan are identical to the reference samples of the 'Indus source'. The composition of the sample taken from the calcareous ooze unit draping the middle Indus Fan (NIOP489/117: open circles) suggests that it is a mixture of fluvial mud and eolian dust ('mixed source'). Filled circles denote the average compositions of the three silt fractions (B, C, D) for the 'Arabian source' and 'Indus source' samples. Data from Prins et al. (2000a).

sediment fraction has been supplied from both source areas ('mixed source').

4.2. Examples of dynamic populations

A variety of sediment types may be present in ocean basins, depending on their location relative to for example major river deltas, deserts and glaciated regions. A selection of genetically distinct sediment types and their production and dispersal mechanisms, combined with examples of modelled EMs from a variety of ocean basins illustrates the DP concept that underlies our analyses (Weltje and Prins, 2001).

4.2.1. Turbidites

Turbidites are produced by redeposition of material that originates by non-selective (slope failure) or selective mechanisms (hyperpycnal flows and other current processes). Transport and deposition are instantaneous and strongly size selective, resulting in a distinctive lithology. Examples of the grain-size variation within two turbidite beds from the Makran continental margin are shown in Fig. 6.

4.2.2. Ice-rafted detritus

Sediment production in glaciated regions is dominated by non-selective production (glacial grinding), although selective production (suspension freezing; Reimnitz et al., 1998) is regionally important. Glacial grinding produces a continuum of particle sizes, while transport by icebergs is en masse and therefore non-selective. Glacial till and iceberg-rafted detritus are characteristically composed of a wide spectrum of grain sizes varying from clay to gravel, pointing to a very low degree of fractionation. An example is shown in Fig. 8D (and in Fig. 10A), where a comparison is made between the ice-rafted EM-1 from the North Atlantic and two glacial till samples.

4.2.3. Contourites

Entrainment of particles by near-bottom currents and deposition from near-bottom currents are both strongly size selective, which results in narrow size distributions that reflect near-bottom current strength (e.g. McCave et al., 1995). An example of two contourite end members from the North Atlantic (Prins et al., 2002) is shown in Fig. 10B. A fundamental problem with hydraulic interpretation of contourite GSDs is the distinction between cases of net deposition and erosion. In the former case, the GSD represents material supplied by and deposited from a near-bottom current, whereas in the latter case, the GSD represents a lag deposit, i.e., material that could not be entrained. Hydraulic interpretation of contourite GSDs is thus restricted to areas of net sediment accumulation.

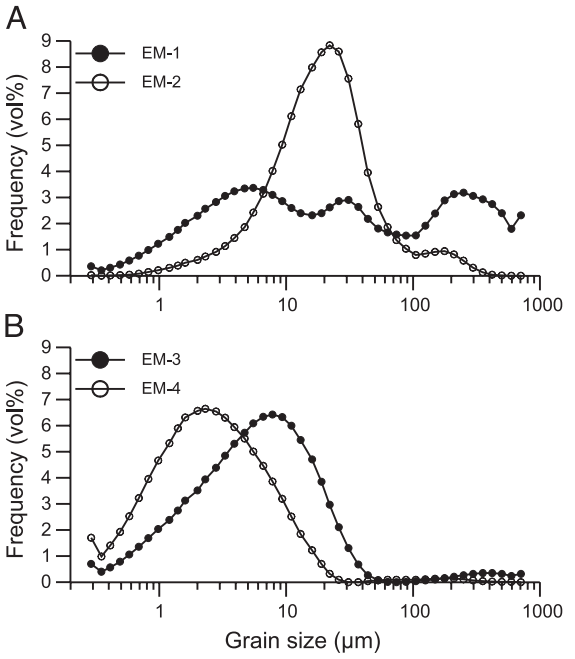

Fig. 10. Grain size distribution of modelled end members in core DS97-2P from Reykjanes Ridge, North Atlantic. (A) EM-1 and EM-2 are related to ice-rafting. (B) EM-3 and EM-4 are contourite GSDs related to near-bottom current activity (Prins et al., 2001, 2002).

4.2.4. Aeolianites

Production of silt-sized aeolianites takes place by a range of processes, including frost shattering, glacial grinding, and impact chipping, which allows for much regional variability in GSDs. Not all of these production mechanisms are selective, so that most selection takes place during entrainment and deposition. Substantial size selection occurs during aeolian transport as very fine-grained dust (phi>8) is lifted into high suspension and separated from coarser material, which is transported over much shorter

distances by either suspension or saltation (e.g. Asslallay et al., 1998). Variations in the GSDs of aeolian sediments in a core at any given locality in the basin reflect contemporaneous wind strength, whereas selective deposition manifests itself as basinward fining of the GSDs at any given time (Figs. 4 and 7). Examples of aeolian end member GSDs are shown in Fig. 8A and B.

4.2.5. Hemipelagites

The bulk of this material is produced by size-selective chemical and physical weathering in coastal lowlands and supplied by fluvial systems. It is transported in the marine environment in the form of flocs and aggregates by a wide variety of sediment dispersal processes (e.g., river plumes, glacier melt-water plumes, and low-density turbidity currents). Although this transport is selective with respect to the composite particles, the expected size distribution of 'elementary' particles within each composite particle is identical. Consequently, one expects the GSD of hemipelagites to be identical throughout the basin in cases where all composite particles have disintegrated, for instance, as a result of sample preparation prior to size analysis. The similarities between the two muddy hemipelagic EMs from the Arabian Sea and the Makran continental margin, and a typical GSD of fluvial mud deposited on the Indus Fan (Fig. 8C) clearly suggest a common production-transport history.

5. Palaeoclimate reconstructions

5.1. High-latitude basin: North Atlantic

The end-member GSD model of the Late Quaternary hemipelagic sediment record in core DS97-2P from Reykjanes Ridge in the North Atlantic (Prins et al., 2001, 2002) is shown in Fig. 10. Four EMs are needed to describe the variation in GSDs within the core.

The two coarsest EMs are interpreted as ice-rafted detritus (Fig. 10A shows EM-1 and EM-2; see also Fig. 8D). EM-1 is a typical example of iceberg-rafted detritus, but the origin of EM-2 is less clear. Observations in the Arctic Ocean indicate that sea ice contains appreciable amounts of predominantly fine-grained sediment. These sediments are incorporated during sea-ice formation in river estuaries and shallow shelf regions of the Arctic Basin by suspension freezing, and by atmospheric deposition during drift (Nürnberg et al., 1994; Lange and Pfirman, 1998; Reimnitz et al., 1998; Hebbeln, 2000). The unimodal ice-rafted EM-2 from the North Atlantic (Prins et al., 2002) might well be an example of material supplied by sea ice, although independent evidence for this is lacking. The IRD was likely supplied by the East Greenland Current (e.g. Moros et al., 1997; Lacksche-

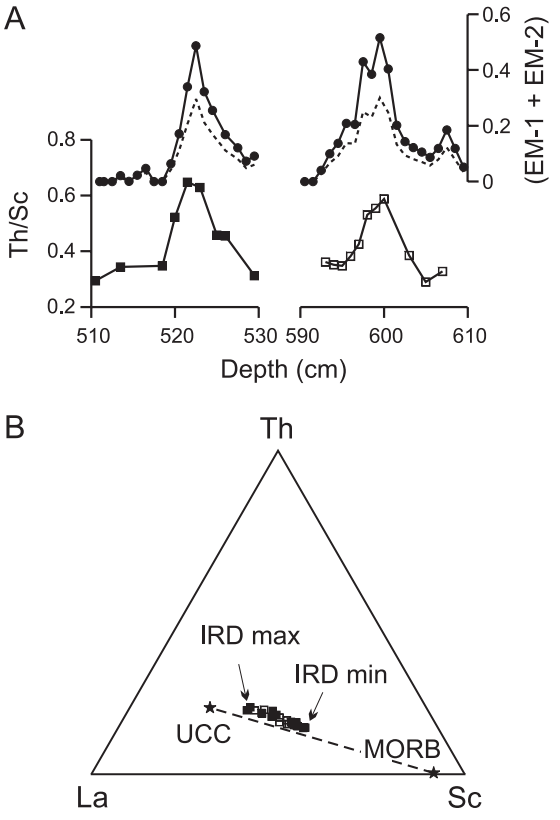

Fig. 11. Trace element geochemistry of the fine silt (<28 μm) fraction in core DS97-2P. (A) Th/Sc ratio in two sections (see Fig. 12), and ice-rafted detritus (IRD) content as inferred from the proportional contribution of EM-1 and EM-2 in bulk terrigenous sediment fraction (solid lines) and in <28 μm fraction (dashed lines). (B) Th–La–Sc composition of the intervals depicted in (A). The mixing line is determined by mid-ocean ridge basalt (MORB) and upper continental crust (UCC) values from the Geochemical Earth Reference Model database (http://www.earthref.org/GERM/). Data from Prins et al. (2002).

witz et al., 1998; Van Kreveld et al., 2000) in the form of icebergs calved from glaciers on eastern Greenland and Iceland.

The well-sorted clayey to fine silty EMs are interpreted as contourites (Fig. 10B shows EM-3 and EM-4) supplied by low-energy bottom currents of the Iceland–Scotland Overflow Water (Lackschewitz et al., 1998; Bianchi and McCave, 2000). Since IRD generally consists of poorly sorted material that may cover the full size range from clay to gravel, it is likely that the clay to silt fraction of the sediments on Reykjanes Ridge consists of a mixture of IRD and contourites. Greenland, the dominant source area of the IRD consists of igneous, sedimentary, and metasedimentary rocks. The area around Iceland, the source of the contourites, is rich in basaltic material related to volcanic activity of the Atlantic mid-ocean ridge. Shifts in mixing proportions of IRD and contourites are therefore expected to coincide with changes in provenance.

A chemical provenance analysis was carried out to examine the validity of the EM model. Prins et al. (2002) analysed the trace element composition of the <28 μm fraction of two sand-rich 20-cm intervals (centred around core depths of 600 and 521 cm), corresponding to large contributions of EM-1 and EM-2. The Th/Sc ratio in both intervals increases simultaneously with the IRD input, from values of ~0.3 to a peak value of ~0.6 (Fig. 11A). The compositions nearly coincide with the binary mixing

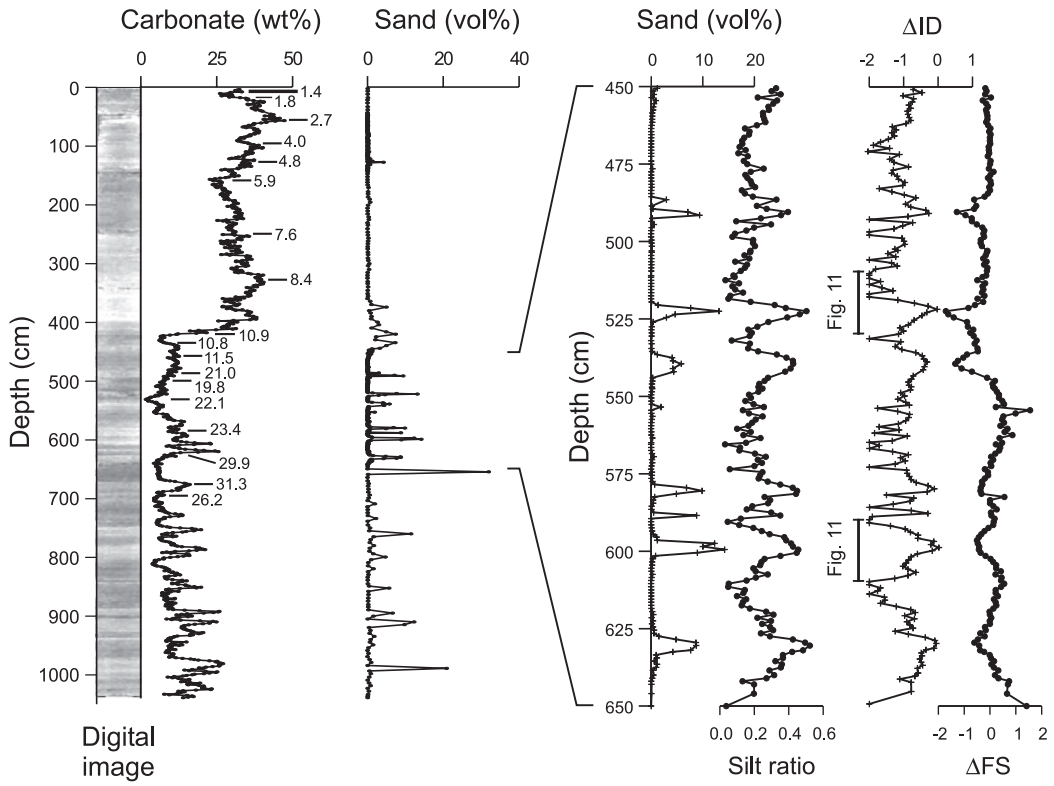

Fig. 12. Core DS97-2P. Carbonate and sand content (fraction >63 μm). Left: digital image illustrates the variations in lithology. Numbers along the carbonate record show ^{14}C ages in ky BP corrected for a −400-year ocean reservoir age. Comparison between sediment composition and end-member contributions in core DS97-2P between 450 and 650 cm: sand content (fraction >63 μm); silt ratio, ratio between 26–63 μm and 9.3–26 μm fractions; ΔID is the log ratio of ((EM-1 + EM-2)/(EM-3 + EM-4)) and is used as indicator of ice-rafted detritus (IRD) content; ΔFS is the log ratio of (EM-3/EM-4) and is used as indicator of Iceland–Scotland Overflow Water (ISOW) flow strength. Data from Prins et al. (2001, 2002).

line between mid-ocean ridge basalt (MORB) and upper continental crust (UCC), when plotted in a Th–La–Sc ternary diagram (Fig. 11B). Calculations based on the Th/Sc reference values for UCC and MORB indicate that the silt fraction within the IRD peaks contains up to 87% of UCC material, in contrast to the IRD-free sediments, which only contain 60–65% of UCC material. The contemporaneous shifts in EM contributions and trace-element composition of the silt fraction confirm the variations in the dominant mode of silt transport to Reykjanes Ridge. It appears that icebergs (and possibly sea ice) supplied predominantly UCC-type materials (East Greenland Current), whereas bottom currents supplied MORB-enriched materials (Iceland–Scotland Overflow Water).

The end-member modelling results have important implications for the use of silt grain size as an indicator for palaeocurrent speed in the glacial North Atlantic. The size distribution within the silt fraction, represented by the ratio of coarse to fine silt, reflects varying bottom-current speed as well as iceberg discharge. In fact, reconstructions of variations in bottom-current speed based on the raw grain-size data (the 'silt ratio') are opposite to inferences from the unmixed record (Fig. 12). The modelling results indicate that the ratio of EM-3 to EM-4 can be used

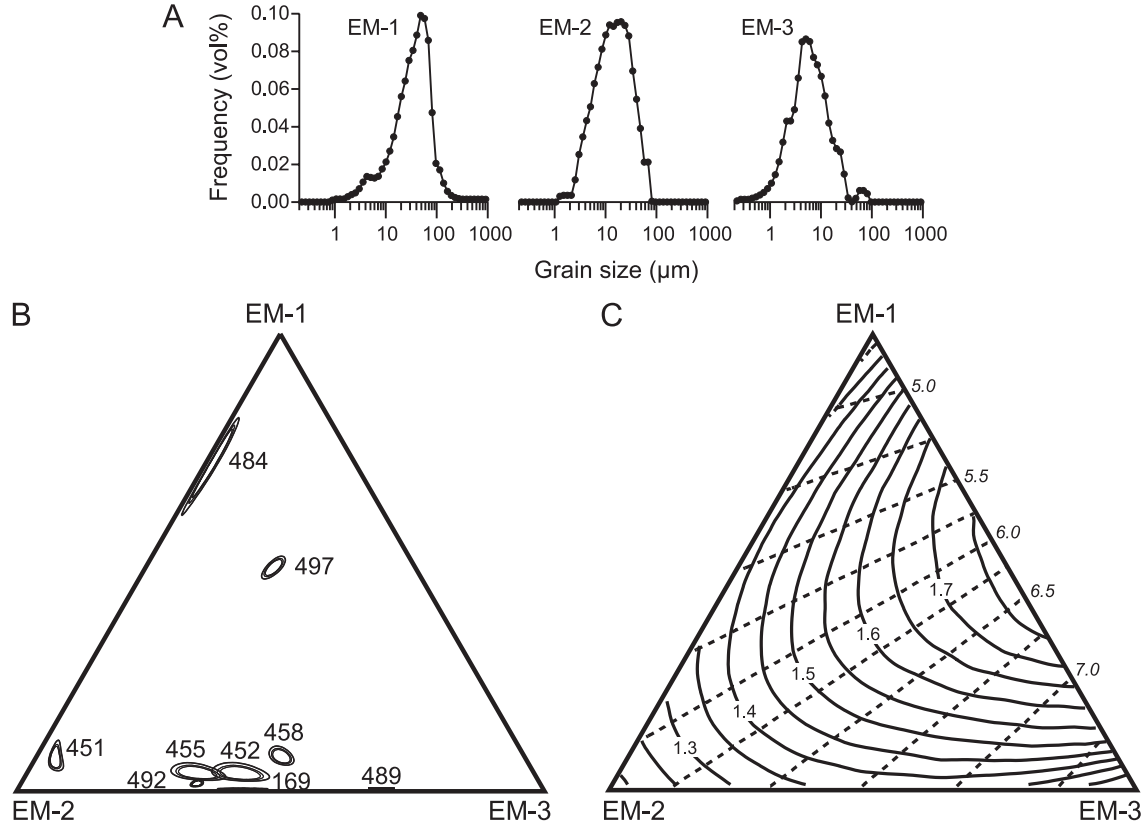

Fig. 13. End-member model of Arabian Sea pelagic and hemipelagic siliciclastic sediments. (A) End member grain-size distributions. Interpretation: EM-1 = coarse aeolian dust; EM-2 = fine aeolian dust; EM-3 = hemipelagic/fluvial mud. (B) Confidence regions (90–95–99%) of population means of sediments cored in the western Arabian Sea (NIOP484, 492, and 497) and the northern and central Arabian Sea (NIOP451, 452, 455, 458, 489, and SO90-169KL) plotted in ternary mixing space (cf. Weltje, 2002). (C) Contour plots of median grain size (dashed lines) and sorting (heavy lines) in ϕ units projected onto mixing space of the three-end-member model. Data from Prins and Weltje (1999).

as an indicator of near-bottom-current speed. The ratio of IRD end members (EM-1 and EM-2) to contourites (EM-3 and EM-4) is used as a measure of iceberg discharge (and possibly sea-ice coverage) relative to near-bottom-circulation strength. The EM model indicates that an increase in grain size within the silt fraction must be attributed to a relative increase in IRD flux and a contemporaneous decrease in deep-ocean circulation. The discrepancy between the interpretations obtained by the conventional approach and EMMA highlights the danger of interpreting grain-size variation in terms of a single controlling factor without knowledge of the sources and dispersal mechanisms of the sediments.

5.2. Low-latitude basin: Arabian Sea

The grain-size distributions of Late Quaternary sediments from the Oman continental slope, the Owen Ridge, the Pakistan continental slope and the Indus Fan can be adequately described as mixtures of three end members (Prins and Weltje, 1999), as shown in Fig. 13A. The total range of compositional variation is visualised in a ternary diagram of which the EMs form the three vertices (Fig. 13B). The individual data points of the estimated compositions of all the samples form a large scatter in the ternary mixing space. When the confidence regions of the mean compositions of each core (cf. Weltje, 2002) are plotted, clear differences emerge between the western and the northern Arabian Sea. Deposition in the western Arabian Sea is dominated by EM-1 and EM-2, which represent coarse and fine aeolian dust. EM-3, which dominates the deposits of the middle Indus Fan and is common on the Pakistan continental slope, represents hemipelagic/fluvial mud (see also Fig. 8B and C).

At any given location, the temporal changes in the relative contribution of the EMs have been interpreted in terms of climate change. The ratio of contributions of coarse to fine aeolian EMs (a measure of the GSD of the aeolian dust) can be used as an indicator of wind strength, and the ratio of contributions of aeolian to fluvial EMs as a measure of continental aridity. Fig. 14 shows the aridity record based on the end-member ratios of core NIOP458 from the upper Indus Fan. Convincing similarities between the planktonic foraminiferal oxygen isotope curve and our grain-size-based climate curve indicate increased continental aridity during glacials (relatively high aeolian dust flux) and increased continental humidity during interglacials (relatively high fluvial mud flux).

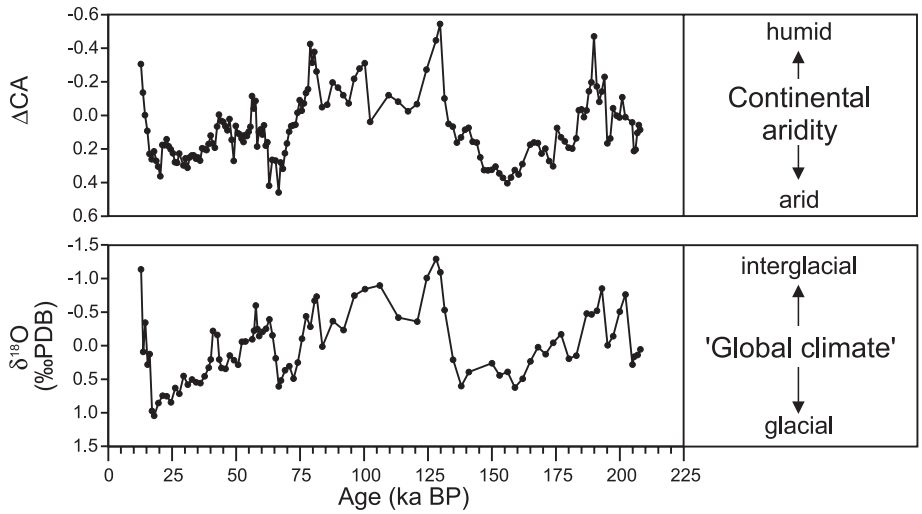

Fig. 14. Late Quaternary reconstruction of variations in Arabian Sea monsoon climate (core NIOP458). Ratio of aeolian to fluvial end-member contributions (ΔCA = log((EM-1 + EM-2)/EM-3)) as indicator for variations in continental aridity. 'Global climate' is indicated by Neogloboquadrina dutertrei $\delta^{18}O$ record. Data from Prins and Weltje (1999).

The inadequacy of univariate GSD statistics for palaeoclimate reconstruction in the Arabian Sea is illustrated in Fig. 13C. Contour lines of median grain size and sorting in ternary space have been constructed for the full range of mixtures of EM-1, EM-2 and EM-3. As shown repeatedly in this study, variations in median size (or in any of the other grain-size statistics) cannot be interpreted unequivocally without knowledge of the end-member GSDs. For instance, a sediment with a median grain size of 6 ϕ could be a mixture of 15% EM-1 and 85% EM-2, or a mixture of 57% EM-1 and 43% EM-3, or a mixture of varying proportions of all three end members. Additional information about the grain-size distribution is needed besides the median grain size to fully characterise the sample. Persistent users of descriptive statistics working in the Arabian Sea are advised to use both the median grain size and the sorting coefficient of the sediment. The location of each observation in the ternary mixing space can be uniquely defined with those two parameters, as shown in Fig. 13C. It is worthwhile to point out that this conclusion could not have been drawn without the existence of the three-end-member model.

5.3. The big picture

The palaeoclimate reconstructions of the North Atlantic Ocean and the Arabian Sea presented above illustrate the common degree of complexity of grain-size records in ocean basins. Fig. 15 shows a comparative palaeoclimate interpretation of the mixing structures in the two basins. Two types of spatio-temporal grain-size variation are present in both ocean basins, one related to provenance (actual mixing) and the other to dispersal (selective deposition). The production and transport mechanisms associated with the four different sediment types are characteristic of high- and low-latitude deep-sea sedimentation patterns. Dominant sediments in the North Atlantic are ice-rafted detritus and contourites, whereas Arabian Sea sediments consist predominantly of aeolian dust and fluvial mud. Both models need two DPs to represent the variations in GSDs resulting from selective dispersal and deposition of sediment associated with changes in atmospheric (Arabian Sea) and oceanic (North Atlantic) circulation. Physical mixing of material from two distinct sources can be expressed as flux ratios (ratios of

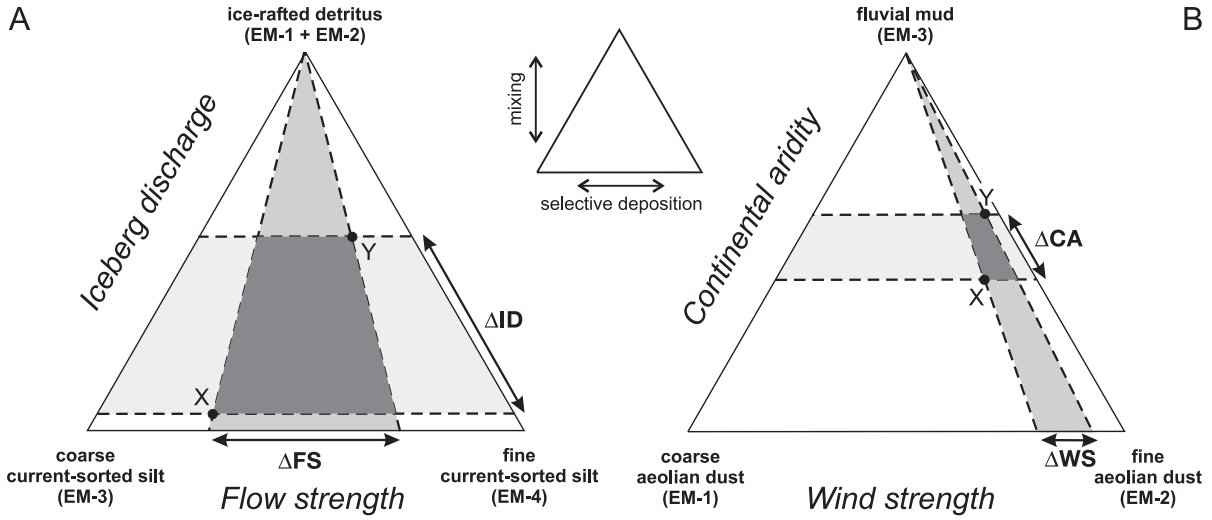

Fig. 15. Ratios of end-member contributions as palaeoclimate indicators. (A) North Atlantic. Variation in near-bottom current flow strength (ΔFS) and iceberg discharge (ΔID) are inferred from the EM-3/EM-4 ratio and (EM-1 + EM-2)/(EM-3 + EM-4) ratio, respectively. X and Y denote peak interstadial and stadial conditions in core DS97-2P. Stadials are characterised by reduced deep-ocean circulation and a relative increase in iceberg discharge. (B) Arabian Sea. Variation in wind strength (ΔWS) and continental aridity (ΔCA) are inferred from the EM-1/EM-2 ratio and (EM-1 + EM-2)/EM-3 ratio, respectively. X and Y denote mean glacial and interglacial conditions in core NIOP458. Glacials are characterised by stronger winter monsoons and increased continental aridity.

mixing coefficients), which may be converted to absolute local fluxes by means of a high-quality age model. In the Arabian Sea, the palaeoclimatic significance of the provenance flux ratio is clear, because it represents the contribution of aeolian (dry) relative to fluvial (wet) sediment input (Fig. 14). Interpretation of the North Atlantic provenance flux ratio is more problematic, because there is as yet no consensus about the palaeoclimatic significance of changes in IRD flux (e.g. Reeh et al., 1999). Sedimentation patterns in both basins are seen to alternate between two states, depicted by X and Y in Fig. 15, which implies that the provenance flux ratio is not independent of circulation strength. This is exactly what one would expect, because both signals are ultimately related to atmospheric and oceanic circulation patterns, which are fully coupled.

6. Discussion and conclusions

In this overview, we have attempted to illustrate the complexity of spatio-temporal variation in GSDs of deep-sea clastics, and shown why simple univariate approaches often fail to provide insights into palaeoclimate. Grain-size variation in deep-sea basins can be adequately described by a spatio-temporal mixing structure, which represents the relative fluxes of a limited number of DPs that typically exhibit unimodal GSDs. Numerical–statistical modelling of the GSDs of deep-marine siliciclastics by EMMA is a powerful method to extract palaeoclimate information from data that can be routinely obtained in nearly every sedimentology lab. The distinction between DPs related to selective dispersal of detritus from a single source, and DPs related to mixing of detritus from different sources is shown to be essential for successful palaeoclimate interpretation. Chemical analysis of specific size fractions, an equally straightforward technique, is a useful tool for interpretation and validation of modelling results. The coupling of end-member GSD models with end-member models of bulk chemistry (or mineralogy) is the obvious next step towards advanced sediment characterisation.

Apart from the possibility of using GSDs for palaeoclimate interpretation, the unravelling of deep-sea grain-size records may have important implications for sediment-transport modelling in general. Our conjecture that many basin fills can be described with a limited number of unimodal DPs implies that a simulation model of fractionated dispersal only needs a limited number of DPs to produce a realistic deep-marine stratigraphy.

The wide range of GSDs of the DPs reconstructed by EMMA clearly illustrates that popular methods of parametric curve fitting do not contribute much to our understanding of the mechanisms governing GSDs of natural sediments. On the contrary, they may obscure the existence of genetically significant subpopulations with GSDs differing markedly from one of the popular theoretical models. The existence of polymodal DPs may simply indicate that certain combinations of non-selective production and transport mechanisms have occurred together (such as glacial grinding and ice rafting), in which case there is no need to decompose the DP into ‘elementary’ subpopulations. Indeed, the GSDs of IRD and tillites exemplify the problematic distinction of genetically meaningful ‘elementary’ subpopulations. The only form of justifiable parametric curve fitting is a method that makes use of adequate process-based models of GSDs, which should ‘... take into account the generation of size distributions from parent rock materials by weathering, the way in which these distributions are modified by transportation and deposition, and the way in which the observed size distribution is generated by the particular methods of measurement and sampling which are used’ (Middleton, 1970). It is clear that this daunting task is far from accomplished, although some progress has been made. We believe that the development of EMMA, a tool with which to explore sets of grain-size data for characteristic DPs, will turn out to be an important part of the groundwork needed to formulate adequate process-based models of GSD.

Acknowledgements

We thank Jef Vandenberghe (Vrije Universiteit, Amsterdam) for permission to use unpublished grain-size data. David Piper and Irina Overeem are thanked for their perceptive reviews, which helped us to clarify the presentation of our ideas. MAP thanks the Earth and Life Sciences council of the Netherlands

Organisation for Scientific Research (NWO-ALW) for financial support.

References

Allen, G.P., Castaing, P., Klingebiel, A., 1971. Preliminary investigation of the surficial sediments in the Cap-Breton Canyon (southwest France) and the surrounding continental shelf. Marine Geology 10, M27–M32.

Allen, G.P., Castaing, P., Klingebiel, A., 1972. Distinction of elementary sand populations in the Gironde estuary (France) by R-mode factor analysis of grain-size data. Sedimentology 19, 21–35.

Ashley, G.M., 1978. Interpretation of polymodal sediments. Journal of Geology 86, 411–421.

Assallay, A.M., Rogers, C.D.F., Smalley, I.J., Jefferson, I.F., 1998. Silt: 2–62 μm, 9–4φ. Earth-Science Reviews 45, 61–88.

Bagnold, R.A., Barndorff-Nielsen, O.E., 1980. The pattern of natural size distributions. Sedimentology 27, 199–207.

Barndorff-Nielsen, O.E., Christiansen, C., 1988. Erosion, deposition and size distributions of sand. Proceedings of the Royal Society 417, 335–352.

Bianchi, G.G., McCave, I.N., 2000. Hydrography and sedimentation under the deep western boundary current on Bjorn and Gardar Drifts, Iceland Basin. Marine Geology 165, 137–169.

Boven, K.L., Rea, D.K., 1998. Partitioning of eolian and hemipelagic sediment in eastern equatorial Pacific core TR 163-31B and the Late Quaternary paleoclimate of the northern Andes. Journal of Sedimentary Research 68, 850–855.

Bridge, J.S., 1981. Hydraulic interpretation of grain-size distributions using a physical model for bedload transport. Journal of Sedimentary Petrology 51 (4), 1109–1124.

Chambers, R.L., Upchurch, S.B., 1979. Multivariate analysis of sedimentary environments using grain-size frequency distributions. Mathematical Geology 11 (1), 27–43.

Christiansen, C., Hartmann, D., 1991. The hyperbolic distribution. In: Syvitski, J.P.M. (Ed.), Principles, Methods, and Applications of Particle Size Analysis. Cambridge Univ. Press, Cambridge, pp. 237–248.

Christiansen, C., Blæsild, P., Dalsgaard, K., 1984. Re-interpreting 'segmented' grain-size distributions. Geological Magazine 121, 47–51.

Clark, M.W., 1976. Some methods for statistical analysis of multimodal distributions and their application to grain-size data. Journal of the International Association for Mathematical Geology 8, 267–282.

Curray, J.R., 1960. Tracing sediment masses by grain size modes. Report of the Twenty-first Session Norden, International Geological Congress, pp. 119–130.

Dacey, M.F., Krumbein, W.C., 1979. Models of breakage and selection for particle size distributions. Journal of Mathematical Geology 11 (2), 193–222.

Dal Cin, R., 1976. The use of factor analysis in determining beach erosion and accretion from grain-size data. Marine Geology 20, 95–116.

Dapples, E.C., 1975. Laws of distribution applied to sand sizes. In: Whitten, E.H.T. (Ed.), Quantitative Studies in the Geological Sciences: A Memoir in Honor of William C. Krumbein. Geological Society of America Memoir, vol. 142, pp. 37–61.

Davis, J.C., 1970. Information contained in sediment-size analyses. Mathematical Geology 2 (2), 105–112.

Davis, J.C., 1986. Statistics and Data Analysis in Geology, 2nd ed. Wiley, New York. 646 pp.

Doeglas, D.J., 1946. Interpretation of the results of mechanical analyses. Journal of Sedimentary Petrology 16 (1), 19–40.

Doeglas, D.J., Brezesinska Smithuysen, W.C., 1941. De interpretatie van de resultaten van korrelgrootte-analysen. Geologie en Mijnbouw 3 (8), 273–285 (pt.1);
Geologie en Mijnbouw 3 (12), 291–302 (pt. 2).

East, T.J., 1985. A factor analytic approach to the identification of geomorphic processes from soil particle size characteristics. Earth Surface Processes and Landforms 10, 441–463.

East, T.J., 1987. A multivariate analysis of the particle size characteristics of regolith in a catchment on the Darling Downs, Australia. Catena 14, 101–118.

Emery, K.O., 1978. Grain size in laminae of beach sand. Journal of Sedimentary Petrology 48, 1203–1212.

Fieller, N.R.J., Flenley, E.C., Olbricht, W., 1992. The statistics of particle size data. Journal of the Royal Statistical Society. Series C, Applied statistics 41, 127–146.

Fillon, R.H., Full, W.E., 1984. Grain-size variations in North Atlantic non-carbonate sediments and sources of terrigenous components. Marine Geology 59, 13–50.

Flemming, B.W., 1988. Process and pattern of sediment mixing in a microtidal coastal lagoon along the west coast of South Africa. In: de Boer, P.L., van Gelder, A., Nio, S.D. (Eds.), Tide-influenced Sedimentary Environments and Facies. Reidel, Dordrecht, pp. 275–288.

Folk, R.L., Ward, W.C., 1957. Brazos River bar: a study in the significance of grain size parameters. Journal of Sedimentary Petrology 27, 3–26.

Forrest, J., Clark, N.R., 1989. Characterizing grain size distributions: evaluation of a new approach using multivariate extension of entropy analysis. Sedimentology 36, 711–722.

Ghosh, J.K., 1988. The sorting hypothesis and new mathematical models for changes in size distribution of sand grains. Indian Journal of Geology 60, 1–10.

Ghosh, J.K., Mazumder, B.S., 1981. Size distribution of suspended particles—unimodality, symmetry, and lognormality. In: Taillie, C., et al. (Eds.), Statistical Distributions in Scientific Work, vol. 6. Reidel, Dordrecht, pp. 21–32.

Grace, J.T., Grothaus, B.T., Ehrlich, R., 1978. Size frequency distributions taken from within sand laminae. Journal of Sedimentary Petrology 48, 1193–1202.

Hartmann, D., Christiansen, C., 1992. The hyperbolic shape triangle as a tool for discriminating populations of sediment samples of closely connected origin. Sedimentology 39, 697–708.

Hebbeln, D., 2000. Flux of ice-rafted detritus from sea-ice in the Fram Strait. Deep-Sea Research. Part 2 47, 1773–1790.

Ibbeken, H., 1983. Jointed source rock and fluvial gravels controlled by Rosin's law: a grain-size study in Calabria, South Italy. Journal of Sedimentary Petrology 53 (4), 1213–1231.

Jöreskog, K.G., Klovan, J.E., Reyment, R.A., 1976. Geological Factor Analysis. Elsevier, Amsterdam. 178 pp.

Kittleman Jr., L.R., 1964. Application of Rosin's distribution in size-frequency analysis of clastic rocks. Journal of Sedimentary Petrology 34 (3), 483–502.

Klovan, J.E., 1966. The use of factor analysis in determining depositional environments from grain-size distributions. Journal of Sedimentary Petrology 36 (1), 115–125.

Komar, P.D., 1986. "Breaks" in grain-size distributions and applications of the suspension criterion to turbidites. Sedimentology 33, 438–440.

Kondolf, G.M., Adhikari, A., 2000. Weibull vs. lognormal distributions for fluvial gravels. Journal of Sedimentary Research 70, 456–460.

Koopmann, B., 1979. Saharastaub in den Sedimenten des subtropisch-tropischen Nordatlantik während den letzten 20.000 Jahre. PhD Thesis. University of Kiel. 109 pp.

Kranck, K., Smith, P.C., Milligan, T., 1996a. Grain-size characteristics of fine-grained unflocculated sediments: I. 'One-round' distributions. Sedimentology 43, 589–596.

Kranck, K., Smith, P.C., Milligan, T., 1996b. Grain-size characteristics of fine-grained unflocculated sediments: II. 'Multi-round' distributions. Sedimentology 43, 597–606.

Krumbein, W.C., 1934. Size frequency distributions of sediments. Journal of Sedimentary Petrology 4, 65–77.

Kuijpers, A., Troelstra, S.R., Prins, M.A., Linthout, K., Akhmetshanov, A., Buryak, S., Bachmann, M.F., Lassen, S., Rasmussen, S., Jensen, J.B., 2003. Late Quaternary sedimentary processes and ocean circulation changes at the Southeast Greenland Margin. Marine Geology 195, 109–129.

Kurashige, Y., Fusejima, Y., 1997. Source identification of suspended sediment from grain-size distributions: I. Application of nonparametric statistical tests. Catena 31, 39–52.

Lackschewitz, K.S., Baumann, K.H., Gehrke, B., Wallrab-Adams, H.J., Thiede, J., Bonani, G., Endler, R., Erlenkeuser, H., Heinemeier, J., 1998. North Atlantic ice sheet fluctuations 10,000–70,000 yr ago as inferred from deposits on the Reykjanes Ridge, southeast of Greenland. Quaternary Research 49, 171–182.

Lange, M.A., Pfirman, S.L., 1998. Arctic sea ice contamination: major characteristics and consequences. In: Leppäranta, M. (Ed.), Physics of Ice-covered Seas: Lecture Notes from a Summer School in Savonlinna, Finland, 6–17 June 1994. Helsinki Univ. Printing House, Helsinki, pp. 651–681.

Leroy, S.D., 1981. Grain size and moment measures: a new look at Karl Pearson's ideas on distributions. Journal of Sedimentary Petrology 51, 625–630.

Lirer, L., Vinci, A., 1991. Grain-size distributions of pyroclastic deposits. Sedimentology 38, 1075–1083.

McCave, I.N., Manighetti, B., Robinson, S.G., 1995. Sortable silt and fine sediment size/composition slicing; parameters for paleocurrent speed and paleoceanography. Paleoceanography 10, 593–610.

Middleton, G.V., 1970. Generation of the log-normal frequency distribution in sediments. In: Romanova, M.A., Sarmanova, O.V. (Eds.), Topics in Mathematical Geology. Consultants Bureau, New York, pp. 34–42.

Middleton, G.V., 1976. Hydraulic interpretation of sand size distributions. Journal of Geology 84, 405–426.

Moreno, A., Cacho, I., Canals, M., Prins, M.A., Sánchez-Goñi, M.-F., Grimalt, J.O., Weltje, G.J., 2002. Saharan dust transport and high-latitude climate variability: the Alboran Sea record. Quaternary Research 58, 318–328.

Moros, M., Endler, R., Lackschewitz, K.S., Wallrabe-Adams, H.-J., Mienert, J., Lemke, W., 1997. Physical properties of Reykjanes Ridge sediments and their linkage to high-resolution Greenland Ice Sheet Project 2 ice core data. Paleoceanography 12, 687–695.

Nürnberg, D., Wollenburg, I., Dethleff, D., Eicken, H., Kassens, H., Letzig, T., Reimnitz, E., Thiede, J., 1994. Sediments in Arctic sea ice: implications for entrainment, transport and release. Marine Geology 119, 185–214.

Orpin, A.R., Woolfe, K.J., 1999. Unmixing relationships as a method of deriving a semi-quantitative terrigenous sediment budget, central Great Barrier Reef lagoon, Australia. Sedimentary Geology 129, 25–35.

Prins, M.A., Weltje, G.J., 1999. End-member modeling of siliciclastic grain-size distributions: the late Quaternary record of eolian and fluvial sediment supply to the Arabian Sea and its paleoclimatic significance. In: Harbaugh, J., et al. (Eds.), Numerical Experiments in Stratigraphy: Recent Advances in Stratigraphic and Sedimentologic Computer Simulations. SEPM (Society for Sedimentary Geology) Special Publication, vol. 62, pp. 91–111.

Prins, M.A., Postma, G., Cleveringa, J., Cramp, A., Kenyon, N.H., 2000a. Controls on terrigenous sediment supply to the Arabian Sea during the late Quaternary: the Indus Fan. Marine Geology 169, 327–349.

Prins, M.A., Postma, G., Weltje, G.J., 2000b. Controls on terrigenous sediment supply to the Arabian Sea during the late Quaternary: the Makran continental slope. Marine Geology 169, 351–371.

Prins, M.A., Troelstra, S.R., Kruk, R.W., Van den Borg, K., De Jong, A.F.M., Weltje, G.J., 2001. The Late Quaternary sedimentary record on Reykjanes Ridge (North Atlantic). Radiocarbon 43 (2B), 939–947.

Prins, M.A., Bouwer, L.M., Beets, C.J., Troelstra, S.R., Weltje, G.J., Kruk, R.W., Kuijpers, A., Vroon, P.Z., 2002. Ocean circulation and iceberg discharge in the glacial North Atlantic: inferences from unmixing of sediment distributions. Geology 30, 555–558.

Rea, D.K., Hovan, S.A., 1995. Grain size distribution and depositional processes of the mineral component of abyssal sediments: lessons from the North Pacific. Paleoceanography 10 (2), 251–258.

Reeh, N., Mayer, C., Miller, H., Thomsen, H.H., Weidick, A., 1999. Present and past climate control on fjord glaciations in Greenland: implications for IRD-deposition in the sea. Geophysical Research Letters 26, 1039–1042.

Reimnitz, E., McCormick, M., Bischof, J., Darby, D.A., 1998. Comparing sea-ice sediment load with Beaufort Sea shelf sediments: is entrainment selective? Journal of Sedimentary Research 68, 777–787.

Sarnthein, M., Tetzlaff, G., Koopmann, B., Wolter, K., Pflaumann, U., 1981. Glacial and interglacial wind regimes over the east-

ern subtropical Atlantic and North-West Africa. Nature 293, 193–196.

Sheridan, M.F., Wohletz, K.H., Dehn, J., 1987. Discrimination of grain-size subpopulations in pyroclastic deposits. Geology 15, 367–370.

Shih, S.M., Komar, P.D., 1994. Sediments, beach morphology and sea cliff erosion within an Oregon coast littoral cell. Journal of Coastal Research 10, 144–157.

Solohub, J.T., Klovan, J.E., 1970. Evaluation of grain-size parameters in lacustrine environments. Journal of Sedimentary Petrology 40 (1), 81–101.

Stuut, J.B.W., Prins, M.A., Schneider, R.S., Weltje, G.J., Jansen, J.H.F., Postma, G., 2002. A 300 kyr record of aridity and wind strength in southwestern Africa: evidence from grain-size distributions of sediments on Walvis Ridge, SE Atlantic. Marine Geology 180, 221–233.

Sun, D., Bloemendal, J., Rea, D.K., Vandenberge, J., Jiang, F., An, Z., Su, R., 2002. Grain-size distribution function of polymodal sediments in hydraulic and aeolian environments, and numerical partitioning of the sedimentary components. Sedimentary Geology 152, 263–277.

Syvitski, J.P.M., 1991. Factor analysis of size frequency distributions: significance of factor solutions based on simulation experiments. In: Syvitski, J.P.M. (Ed.), Principles, Methods, and Applications of Particle Size Analysis. Cambridge Univ. Press, Cambridge, pp. 249–263.

Tanner, W.F., 1958. Modification of sediment size distributions. Journal of Sedimentary Petrology 34 (1), 156–164.

Van Kreveld, S., Sarnthein, M., Erlenkeuser, H., Grootes, P., Jung, S., Nadeau, M.J., Pflaumann, U., Voelker, A., 2000. Potential links between surging ice sheets, circulation changes, and the Dansgaard–Oeschger cycles in the Irminger Sea, 60–18 kyr. Paleoceanography 15, 425–442.

Visher, G.S., 1969. Grain size distributions and depositional processes. Journal of Sedimentary Petrology 39 (3), 1074–1106.

Weltje, G.J., 1995. Unravelling mixed provenance of coastal sands: the Po delta and adjacent beaches of the northern Adriatic Sea as a test case. In: Oti, M.N., Postma, G. (Eds.), Geology of Deltas. Balkema, Rotterdam, pp. 181–202.

Weltje, G.J., 1997. End-member modeling of compositional data: numerical–statistical algorithms for solving the explicit mixing problem. Journal of Mathematical Geology 29, 503–549.

Weltje, G.J., 1998. Compositional and textural heterogeneity of detrital sediments: towards a quantitative framework for sedimentary petrology. In: Buccianti, A., Nardi, G., Potenza, R. (Eds.), Proceedings of IAMG'98—The Fourth Annual Conference of the International Association for Mathematical Geology, vol. 1. De Frede Editore, Napoli, pp. 65–70.

Weltje, G.J., 2001. Decomposing compositions: minimum chi-squared reduced-rank approximations on the simplex. Proceedings of the 2001 Annual Conference of the International Association for Mathematical Geology (IAMG), Cancún, Mexico, 6–12 September 2001. http://www.kgs.ukans.edu/Conferences/IAMG/Sessions/L/weltje.html.

Weltje, G.J., 2002. Quantitative analysis of detrital modes: statistically rigorous confidence regions in ternary diagrams and their use in sedimentary petrology. Earth-Science Reviews 57, 211–253.

Weltje, G.J., Prins, M.A., 2001. Sources and dispersal patterns of deep-marine siliciclastics: inferences from end-member modeling of grain-size distributions. Proceedings of the 2001 Annual Conference of the International Association for Mathematical Geology (IAMG), Cancún, Mexico, 6–12 September 2001. http://www.kgs.ukans.edu/Conferences/IAMG/Sessions/B/weltje.html.

Wohletz, K.H., Sheridan, M.F., Brown, W.K., 1989. Particle size distributions and the sequential fragmentation/transport theory applied to volcanic ash. Journal of Geophysical Research 94 (B11), 15703–15721.

Zhou, D., Chen, H., Lou, Y., 1991. The log-ratio approach to the classification of modern sediments and sedimentary environments in northern South China Sea. Mathematical Geology 23, 157–165.